First-principle molecular dynamics study of bond disruption and formation in SiO 2 upon irradiation

ARTICLE *in* PHYSICA B CONDENSED MATTER · APRIL 2006

Impact Factor: 1.32 · DOI: 10.1016/j.physb.2005.12.235

4 AUTHORS, INCLUDING:

Mauro Boero
Institut de Physique et Chimie des Matériau…
187 PUBLICATIONS **3,475** CITATIONS

SEE PROFILE

Atsushi Oshiyama
The University of Tokyo
266 PUBLICATIONS **8,743** CITATIONS

SEE PROFILE

Pier Luigi Silvestrelli
University of Padova
93 PUBLICATIONS **3,286** CITATIONS

SEE PROFILE

Available online at www.sciencedirect.com
SCIENCE DIRECT
Physica B 376–377 (2006) 945–949
PHYSICA B
www.elsevier.com/locate/physb

First-principle molecular dynamics study of bond disruption and formation in SiO_2 upon irradiation

Mauro Boero[a,*], Atsushi Oshiyama[b], Pier Luigi Silvestrelli[c], Kouichi Murakami[d]

[a]*Center for Computational Sciences, University of Tsukuba, 1-1-1 Tennodai, Tsukuba, Ibaraki 305-8571, Japan*
[b]*Institute of Physics, University of Tsukuba, 1-1-1 Tennodai, Tsukuba, Ibaraki 305-8571, Japan*
[c]*DEMOCRITOS National Simulation Center, Trieste, Italy and Dip. di Fisica "G. Galilei", Università di Padova, via Marzolo 8, I-35131 Padova, Italy*
[d]*Institute of Applied Physics, University of Tsukuba, 1-1-1 Tennodai, Tsukuba, Ibaraki 305-8573, Japan*

Abstract

Recent experiments have shown that Si nanostructures can be formed in a matrix of SiO_2 by laser-pulse irradiation, with appealing applications in nanotechnology. We hereby present first principles simulations that provide a microscopic insight into the underlying mechanism, showing how electron excitations weaken Si–O bonds in SiO_2, dislodging O atoms and allowing the formation of stable Si–Si structures below the melting temperature.

PACS: 71.15.Pd; 71.55.−i; 76.30.−v

Keywords: Free energy; Molecular dynamics; Silicon dioxide; Silicon

1. Introduction

Silicon is a fundamental material in the present semiconductor technology. Yet, in the perspective of further miniaturization, driven by the emerging nanotechnology, new synthesis methods, suitable to realize Si nanowires and nanodots on a SiO_2 substrate, are required. Ion implantation [1] has been used to create small Si islands in SiO_2. However, its drawback is that it can affect only surface regions $\leqslant 1\,\mu m$ for an incident ion beam of about 1 MeV. To make technologically appealing Si patterns, focused Si^+ ion beams must be used, but it is difficult to produce high current beams and it takes a very long time to write a Si pattern. Furthermore, the energy of the incident ions in focused beams is 10–100 keV, thus the Si thickness drops to ~10 nm.

A very recent set of experiments has evidenced more interesting ways to create Si nanocrystals in SiO_2 without reaching the melting point ($T_{melting} = 1883\,K$) and without requiring the high energies of the ion implantation. Namely, by immersing a pristine SiO_2 sample in a molten $CaCl_2$ salt at 1123 K and injecting an electric current through a metal wire, the oxygen of the SiO_2 sample is released into the salt as oxide ions and on that spot Si islands can be created [2]. If the wire is thin enough, the size of the islands can be controlled with evident technological implications. An alternative—and equally appealing—technique consists in irradiating silica with femtosecond laser pulses [3,4]. In the spots where the laser beam touches a SiO_2 sample, fingerprints peculiar of Si crystallization in SiO_2 have been shown. In the process, the irradiated spots are likely to undergo a phase transition to a liquid state or, alternatively, to a solid plasma state and then revert back to the solid state upon cooling. Oxygen atoms are expected to diffuse away from the irradiated nano-areas to be trapped at more distant regions or to leave the surface as gas phase molecules. At very low laser fluences, it has also been observed that femtosecond laser irradiation induces an enhancement of the refractive index of SiO_2. This has been ascribed to strong changes in the Si–O–Si bond angles, resulting as a consequence of local formation of Si–Si bonds via Si–O bond breaking [4].

*Corresponding author. Tel.: +81 29 853 5921; fax: +81 29 853 5924.
E-mail address: boero@comas.frsc.tsukuba.ac.jp (M. Boero).

0921-4526/$ - see front matter © 2006 Elsevier B.V. All rights reserved.
doi:10.1016/j.physb.2005.12.235

Although at a pioneering stage, these techniques represent a promising tool to create Si nanostructures in a matrix of SiO_2 in a controlled way. Indeed, laser irradiation has become a versatile tool to manipulate chemical bonds of various elements [5,6] or to generate a short-living liquid states in a solid [4,7,8]. Upon laser irradiation, electrons are excited and these excitations, although below the energy gap ($\hbar\omega < E_{gap}$) of the material, can promote the formation of Si–Si bonds. As a general picture, electrons are excited, then equilibrate on a femtosecond time scale, and this induces atomic displacements leading to the (re)crystallization of the material. To probe this picture, we present simulations performed on a bulk sample of SiO_2 within the ab initio free energy molecular dynamics (FEMD) method [9], suitable to treat laser excitation phenomena [10–12] in which the electronic degrees of freedom are not on the ground state. On one hand, we want to identify which states are realized upon electron excitation, namely at which values of $\hbar\omega$ a liquid or a solid plasma state is formed and when, instead, no phase transitions occur (solid phase below $T_{melting}$). On the other hand, we try to gain an atomistic insight into the formation of Si–Si bonds upon irradiation. Indeed, by changing $\hbar\omega$ between 1.7 and 2.6 eV, i.e. the electronic temperature $T_e = \hbar\omega/k_B$, we found that in a certain range of T_e, although the ionic temperature T_I is still below $T_{melting}$, a substantial amount of Si–Si bonds is formed and these bonds are dynamically stable [13]. This offers a clue to understand which range of electron excitations promote the formation of the Si bonds, without melting or damaging the pristine SiO_2 sample, and how the formation of the seeds of Si nanocrystals proceeds. Last, but not least, we have also found that an oxygen-deficient center (ODC), which is the most abundant defect in SiO_2, enhances the formation of the Si seeds and the recrystallization of the structure.

2. Computational details

In our FEMD simulations [14], the ions are allowed to evolve freely while the electrons are kept at a given T_e. The electron density is written in terms of single particle orbitals,

$$\rho(\mathbf{x}) = \sum_{i=1}^{N_{max}} f_i |\psi_i(\mathbf{x})|^2 \quad (1)$$

and the occupation numbers are given by the Fermi–Dirac statistics $f_i = [e^{(E_i-\mu)/k_B T_e} + 1]^{-1}$ with N_{max} determined by the condition $f_i > 10^{-6}$, necessary to include a sufficiently large number of (numerically) unoccupied states. This electron density is computed at each step during the dynamics by minimizing the free energy functional [9]

$$F = \Omega[\rho(\mathbf{x})] + \mu N_e + E_{II} \quad (2)$$

where

$$\Omega[\rho(\mathbf{x})] = -2k_B T_e \ln \det[1 + e^{-(H-\mu)/k_B T_e}] - \int \rho(\mathbf{x}) \left[\frac{V_H(\mathbf{x})}{2} + \frac{\delta E_{xc}}{\delta\rho(\mathbf{x})}\right] d^3x + E_{xc}, \quad (3)$$

H is the effective one-electron hamiltonian, V_H the Hartree potential, E_{xc} the exchange-correlation in the formulation of Perdew et al. [15], and E_{II} the ion–ion Coulomb energy. The core-valence interactions are described by Troullier–Martins norm-conserving pseudopotentials [16]. Valence wavefunctions are expanded in plane waves with an energy cut-off of 70 Ry. The simulated system consists of an α-quartz tetragonal supercell of $9.832 \times 8.514 \times 10.811$ Å^3, built from the experimental lattice parameters, and containing 24 formula units (Fig. 1(a)). Periodic boundary conditions are applied and the Brillouin zone is sampled only at the Γ point [10]. Dynamical simulations were performed on a (N, V, E) ensemble, the electronic temperature T_e was set to three different values (20 000, 25 000 and 30 000 K) corresponding to three different excitation energies (1.72, 2.16 and 2.59 eV, respectively) and an ionic integration time step of 50 a.u. (1.2 fs) was adopted.

3. Results and discussion

After a standard geometry relaxation of the SiO_2 system, to get a stress-free initial configuration (Fig. 1(a)), we set T_e to 20 000 K and allowed the system to evolve freely for about 1.2 ps, sufficient to reach a dynamical equilibrium. The fact that the electrons are *hot* originates forces acting on the atoms that are drastically different from those of a ground state calculation. Yet, the femtosecond time scale of the electron relaxation is much shorter than the electron–ion relaxation time $\tau_{eI} \sim 1$ ps [17] and this allows to treat electrons and ions in an *adiabatic* way. The ionic temperature oscillates around 304 K (Fig. 2) and the atomic displacements monitored along the trajectory are typical of a SiO_2 crystal at room temperature. No noticeable electronic or structural changes were observed at this T_e as evidenced by the density of states (DOS) and by the pair correlation functions (PCF) (Figs. 3 and 4) that show only the typical features of regular α-quartz.

A second simulation was started from the same initial relaxed configuration, setting $T_e = 25\,000$ K. The forces $\nabla_{\mathbf{R}_I} F$ acting on the ions change as a response to the modification of the electron density $\rho(\mathbf{x})$, depending on T_e both via the occupation numbers f_i and the related redistribution of the energy eigenvalues E_i and orbitals ψ_i. After an initial large oscillation, a new equilibrium is attained in about 1.9 ps. The average ionic temperature is $T_I = 367$ K and still below $T_{melting}$ (Fig. 2). Nevertheless, the increased electronic temperature is now sufficient to induce a weakening of several Si–O bonds, with large structural oscillations that in some cases result in a Si–O bond breaking. The equilibration time, longer than in the previous case, reflects the fact that the structure now

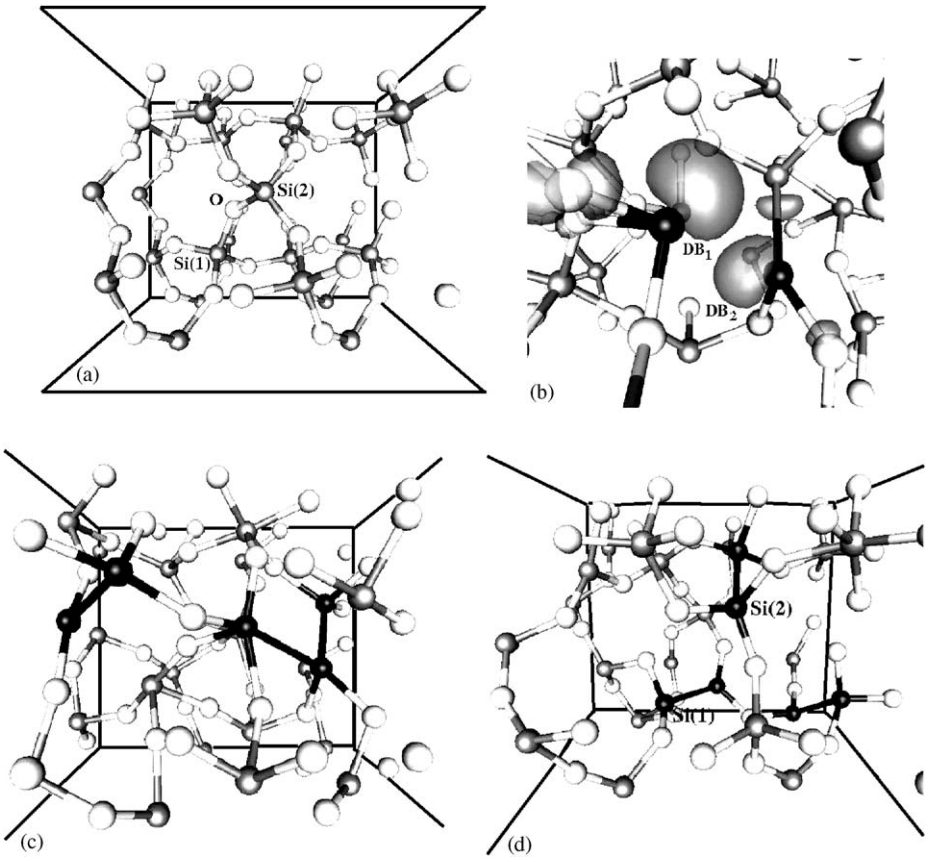

Fig. 1. (a) SiO_2 supercell. Si and O atoms are the gray and white balls, respectively. (b) Detail of an intermediate configuration at $T_e = 25\,000$ K with two DB (DB_1, DB_2) ready to form a Si–Si bond (the two black Si). Isosurfaces (gray): $|\psi_i|^2 = 5 \times 10^{-3}$ Å^{-3}. (c) Equilibrated structure at $T_e = 25\,000$ K with the stable Si–Si bonds in black. (d) Equilibrated ODC structure at $T_e = 25\,000$ K. (Si–Si bonds in black).

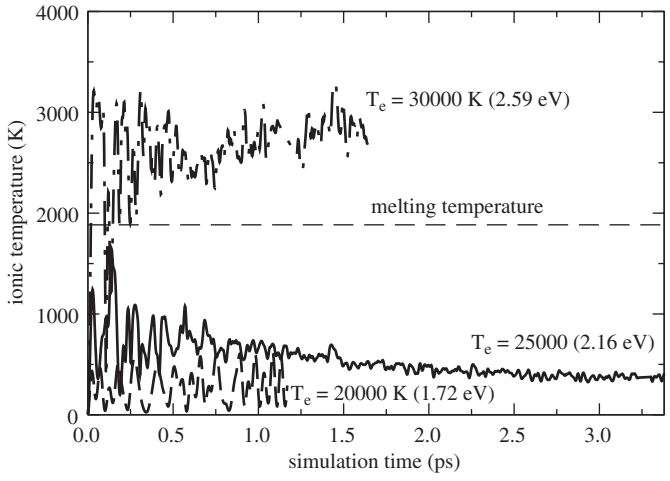

Fig. 2. Evolution of the ionic temperature at the three electronic temperatures simulated for case of the perfect α-quartz crystal.

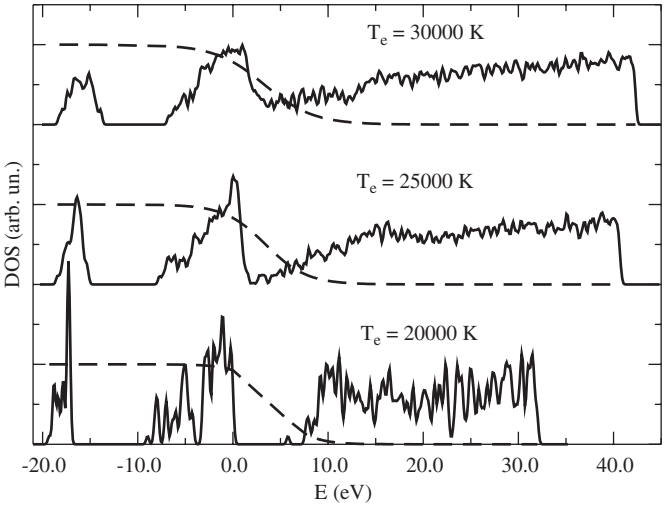

Fig. 3. Electronic density of states (DOS) for the three different T_e values, computed by averaging on the final equilibrated systems. The superposed dashed lines show the fermionic distributions of the occupation numbers f_i.

undergoes profound modifications by breaking bonds and forming new ones. The stabilization occurs via formation of new bonds and, among regular Si–O, few Si–Si bonds appeared.

Since it is easier for O to break its two bonds with Si rather than for Si to break all its four bonds, O atoms can be dislodged from their position and can migrate elsewhere. The diffusion coefficients of the two species were computed via the standard velocity–velocity

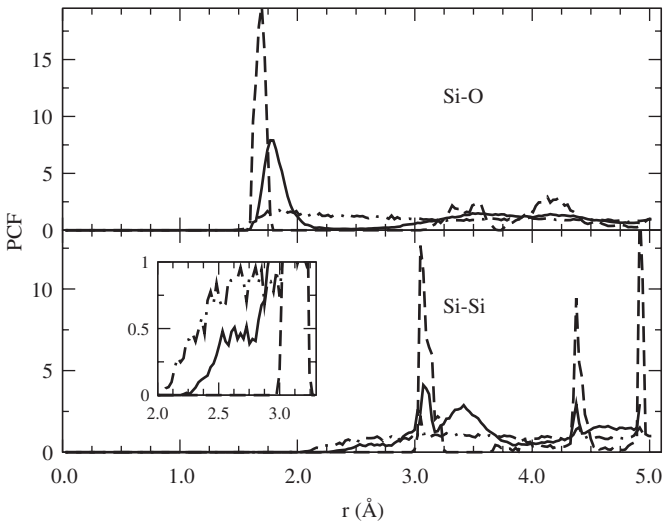

Fig. 4. Si–O (upper panel) and Si–Si (lower panel) pair correlation functions (PCF) for $T_e = 20\,000$ K (dashed line), 25 000 K (solid line) and 30 000 K (dot–dashed line). The inset shows the details between 2.0 and 3.5 Å of the Si–Si PCF.

autocorrelation formula

$$D_s = \frac{1}{3}\int_0^\infty \frac{1}{N_s}\sum_{I=1}^{N_s} \langle \mathbf{v}_{I,s}(t)\mathbf{v}_{I,s}(0)\rangle \, dt \quad (4)$$

with $s = \mathrm{Si}, \mathrm{O}$, and show that the diffusion of O ($D_O = 8.49 \times 10^{-9}\,\mathrm{cm}^2/\mathrm{s}$) is about a factor two larger than Si ($D_{Si} = 4.09 \times 10^{-9}\,\mathrm{cm}^2/\mathrm{s}$) [13]. The O activation energy ($E_a = 1.36$ eV), estimated by Arrhenius plot fitting, is in agreement with both experiment [18] and theory [19]. However, this comparison must be taken with some care, since we deal with excited electrons, while Ref. [19] is a ground state calculation.

The weakening of the Si–O bonds occurs in regions where the electron excitations localize. In fact, by monitoring the DOS and the electronic states (Fig. 1(b)), we see that when an O atom diffuses away, it leaves behind two Si sp^3 DBs that are located in energy at ~2.7–3.0 eV above the highest occupied state of SiO_2, i.e. inside the SiO_2 gap, and are characterized by occupation numbers $f_i = 0.86$ and 0.82 respectively. These DBs resemble E' centers [20–22] and since they are so close, the system reconstructs by forming a Si–Si dimer with a length of 2.54 ± 0.08 Å. Once formed, the dimer is stable on the time scale of the simulation. The gap states corresponding to the former DBs disappear and the electron density shows the typical shape of an actual Si–Si covalent bond. The final equilibrated structure is shown in Fig. 1(c). The total number of Si atoms forming stable Si–Si bonds, with lengths ranging from 2.51 to 2.64 Å, is ~20% of the total number of Si in the supercell. This results in non-zero values around 2.6 Å of the Si–Si PCF (Fig. 4). Analogously, the broad peak at ~3.4 Å is due to ≡Si−Si−O−Si≡ and ≡Si−Si−Si≡ structures. Analogously, the presence of ≡Si−Si−O− structures is responsible for a shift toward 1.78 Å and a broadening of the first peak of the Si–O PCF. Although $T_I < T_{melting}$, the formation of Si–Si bonds is promoted by strong lattice distortions induced by the weakening of the chemical bonds. Since we are working in a microcanonical ensemble, an O atom that leaves a ≡Si−O−Si≡ bridge is simply displaced elsewhere in the network and forms three-membered ring structure in which a 3-fold O atom and Si floating bonds (FB) co-exist. These structures have been shown to be typical in SiO_2 [21,23], hence they are not an artifact of the simulation.

When T_e was raised to 30 000 K, the ionic forces became so large that the system went above the melting point in about 0.3 ps, equilibrating at $T_I = 2870$ K (Fig. 2). The PCFs are almost structureless with only a signature of a dynamical Si–O short range order (Fig. 4) and analysis of the trajectory shows that chemical bonds are continuously broken and reformed. A large amount of unbound atoms wander around and the energy gap (Fig. 3) is filled by a large population of unsaturated bonds, typical of the liquid state of SiO_2 [24], while diffusion coefficients increase dramatically ($D_{Si} = 1.42 \times 10^{-7}$ and $D_O = 3.40 \times 10^{-7}\,\mathrm{cm}^2/\mathrm{s}$). This is in agreement with the transient liquid state observed in high frequency irradiation [7,8].

Finally, we examined an oxygen deficient center (ODC) by removing the O atom of the ≡Si(1)−O−Si(2)≡ bridge (Fig. 1(a)). This is the most common point-like defect in α-quartz and leaves the system with a neutral vacancy of the type ≡Si(1)$^\bullet$ $^\bullet$Si(2)≡ in which two Si sp^3 DBs face each other. In the first simulation, we set $T_e = 20\,000$ K and a FEMD run was performed for about 0.55 ps. Under these conditions, the two Si atoms facing the O vacancy dimerize in ~0.1 ps, forming a Si–Si bond of 2.53 ± 0.12 Å. This is the only Si–Si bond formed at this T_e. T_I stabilizes around 300 K and the main parameters of the simulation do not differ significantly from the perfect crystal.

Instead, when we increased T_e to 25 000 K, in the first stage (~0.1 ps), Si(1) and Si(2) form a dimer; this turns out to be an unstable structure that undergoes a very quick breaking. Indeed, after about 0.13 ps, Si(2) moves beyond the plane of its neighbor O atoms as in a puckering configuration [20,22], forming a new bond with a nearby oxygen. Meanwhile, Si(1) survives temporarily as an unpaired DB. This corresponds to a metastable puckering configuration which has already been found to be typical of either a charged [20] or excited [21] oxygen vacancies. From this point on, the evolution of the ODC system follows a pathway very similar to the case of the undefective α-quartz. The ionic temperature oscillates around 490 K while O atoms are dislodged, bonds are broken and new Si–O and Si–Si bonds are formed. Eventually, the system reaches a stable average configuration shown in Fig. 1(d). Four stable Si–Si bonds (~25% of the total number of Si atoms) with average distances ranging from 2.56 to 2.39 Å were formed in the regions where localized excitations induce a Si–O bond weakening, with subsequent departure of O atoms. At the equilibrium, neither ≡Si−O$^\bullet$ nor DBs survive, but three-membered rings [23] and FBs [13]. The

amount of Si–Si bonds formed in the presence of an ODC (25%) is larger than in pristine SiO_2 (20%), indicating that the removal of oxygens enhances the formation of Si nanocrystals.

4. Conclusions

The present work offers a microscopic picture in the formation of Si–Si bonds in a matrix of in SiO_2 upon fast electron excitations. In particular, we have shown how excitations characterized by $\hbar\omega$ values below the energy gap of SiO_2 can promote DBs formation and induce structural modifications without requiring melting conditions. The amount Si–Si bonds created represents a substantial percentage of the Si atoms of the system and, once that they are created, they are stable. At $\hbar\omega \geqslant 2.59\,\text{eV}$ a liquid state is obtained, due to the increase of the forces acting on the ions and the related electronic structure modifications responsible for the weakening of the chemical bonds.

Acknowledgements

We acknowledge support from Special Nanoscience Project—Tsukuba University and ACT-JST Program.

References

[1] A.P. Baraban, D.V. Egorov, Y.V. Petrov, L.V. Miloglyadova, Tech. Phys. Lett. 30 (2004) 85.
[2] T. Nohira, K. Yasuda, Y. Ito, Nature Mater. 2 (2003) 397.
[3] K. Hirao, Internal Modifications inside Glasses with a Femtosecond Pulse Laser, Japan Society of Applied Physics on 64th Autumn Meeting, Ext. Abstract 31p-F-6, 2003.
[4] N. Fukata, Y. Yamamoto, K. Murakami, M. Hase, M. Kitajima, Appl. Phys. Lett. 87 (2003) 3495.
[5] K. Sokolowski-Tinten, C. Blome, C. Dietrich, A. Tarasevitch, M. Horn von Hoegen, D. von der Linde, Phys. Rev. Lett. 87 (2001) 225701.
[6] M. Garavelli, P. Celani, N. Yamamoto, F. Bernardi, M.A. Robb, M. Olivucci, J. Am. Chem. Soc. 118 (1996) 11656.
[7] K. Murakami, H.C. Gerristen, H. van Brug, F. Bijkerk, F.W. Saris, M.J. van der Wiel, Phys. Rev. Lett. 56 (1986) 655.
[8] L. Huang, J.P. Callan, E.N. Glezer, E. Mazur, Phys. Rev. Lett. 80 (1998) 185.
[9] A. Alavi, J. Kohanoff, M. Parrinello, D. Frenkel, Phys. Rev. Lett. 73 (1994) 2599.
[10] P.L. Silvestrelli, A. Alavi, M. Parrinello, D. Frenkel, Phys. Rev. Lett. 77 (1996) 3149.
[11] P.L. Silvestrelli, A. Alavi, M. Parrinello, D. Frenkel, Phys. Rev. B 56 (1997) 3806.
[12] P.L. Silvestrelli, M. Parrinello, J. Appl. Phys. 83 (1998) 2478.
[13] M. Boero, A. Oshiyama, P.L. Silvestrelli, K. Murakami, Appl. Phys. Lett. 86 (2005) 201910.
[14] CPMD code by J. Hutter, et al., Max-Planck-Institut FKF and IBM Zurich Research Laboratory, 1995–2004.
[15] J.P. Perdew, K. Burke, M. Ernzerhof, Phys. Rev. Lett. 77 (1996) 3865.
[16] N. Troullier, J.L. Martins, Phys. Rev. B 43 (1991) 1993.
[17] K. Seibert, G.C. Cho, W. Kütt, H. Kurz, D.H. Reitze, J.I. Dadap, H. Ahn, M.C. Downer, A. Malvezzi, Phys. Rev. B 42 (1990) 2842.
[18] M.A. Lamkin, F.L. Riley, R.J. Fordham, J. Eur. Ceramic Soc. 10 (1992) 347.
[19] D.R. Hamann, Phys. Rev. Lett. 81 (1988) 3447.
[20] M. Boero, A. Pasquarello, J. Sarnthein, R. Car, Phys. Rev. Lett. 78 (1997) 887.
[21] M. Boero, A. Oshiyama, P.L. Silvestrelli, Phys. Rev. Lett. 91 (2003) 206401.
[22] M. Boero, A. Oshiyama, P.L. Silvestrelli, Mod. Phys. Lett. B 18 (2004) 707.
[23] P. Umari, X. Gonze, A. Pasquarello, Phys. Rev. Lett. 90 (2003) 027401.
[24] A. Trave, P. Tangney, S. Scandolo, A. Pasquarello, R. Car, Phys. Rev. Lett. 89 (2002) 245504.